Effects of CO2 vegetation forcing on precipitation and heat extremes in China

Zheng Chen (chenzh21@lzu.edu.cn)
Lanzhou University College of Atmospheric Sciences https://orcid.org/0000-0002-1970-5524
Xin-Tong Hou
Lanzhou University College of Atmospheric Sciences
Pei-Yi Fan
Lanzhou University College of Atmospheric Sciences
Fei Ji
Lanzhou University College of Atmospheric Sciences
Li Li
Shanxi University
Gui-Quan Sun
North University of China
Guo-Lin Feng
Lanzhou University College of Atmospheric Sciences
Zhong-Hua Qian
Yangzhou University School of Physical Science and Technology

---

Research Article

Keywords: anthropogenic activities, land-atmosphere feedback, vegetation forcing, extreme events

Posted Date: June 20th, 2023

DOI: https://doi.org/10.21203/rs.3.rs-3023943/v1

Version of Record: A version of this preprint was published at Climate Dynamics on December 22nd, 2023. See the published version at https://doi.org/10.1007/s00382-023-07046-5.

Effects of CO_2 vegetation forcing on precipitation and heat extremes in China

Zheng Chen[1], Xin-Tong Hou[1], Pei-Yi Fan[1], Fei Ji[1], Li Li[3], Gui-Quan Sun[4,5], Guo-Lin Feng[1,2,6*], Zhong-Hua Qian[2*]

[1]College of Atmospheric Sciences, Lanzhou University, Lanzhou, 730000, Gansu, China.
[2]School of Physics Science and Technology, Yangzhou University, Yangzhou, 225002, Jiangsu, China.
[3]School of Computer and Information Technology, Shanxi University, Taiyuan, 030006, Shanxi, China.
[4]Department of Mathematics, North University of China, Taiyuan, 030051, Shanxi, China.
[5]Complex Systems Research Center, Shanxi University, Taiyuan, 030006, Shanxi, China.
[6]Laboratory for Climate Studies, National Climate Center, Beijing, 100081, Shanxi, China.

*Corresponding author(s). E-mail(s): fenggl@cma.gov.cn; qianzh@yzu.edu.cn;

Abstract

Anthropogenic CO_2 emissions are expected to significantly impact climate patterns, including extreme heat events. The influence of plants on land-atmosphere water and energy exchanges plays a crucial role in shaping these heat extremes. The response of vegetation growth and physiology to elevated CO_2, both directly and indirectly, will determine their contribution to future heat extremes. In this study, we employed a suite of CMIP6 earth system models (ESMs) to differentiate between the effects of radiative forcing and vegetation forcing under elevated CO_2 background on extreme heat and precipitation events in China. The changes observed can be attributed to CO_2 physiological forcing, which reduces transpiration and its related cooling impact, leading to a decrease in clouds and precipitation under $2\times CO_2$ and $4\times CO_2$ scenarios. Our findings indicate that CO_2-induced vegetation forcing (VEG) intensifies the frequency and severity of future heatwaves. Additionally, we found that CO_2-driven vegetation decreases extreme precipitation and increases dry days numbers in most humid regions of China, despite the increase in transpiration resulting from the saving of soil moisture and aboveground biomass enhancement due to $\mathbf{CO_2}$ fertilization.

Keywords: anthropogenic activities, land-atmosphere feedback, vegetation forcing, extreme events

1 Introduction

Amidst the context of global warming, extreme events are becoming increasingly common worldwide and have had a significant impact on human society [1–3]. For example, real extreme heat waves can lead to crop reduction [4], reduced net primary productivity of vegetation [5], and even the death of organisms. Similarly, in China, extreme heat waves and extreme precipitation can cause incalculable losses [6, 7].

The IPCC has confirmed that the primary driver of current climate change is the increase in anthropogenic CO_2 emissions. Besides acting as a greenhouse gas, CO_2 has an indirect impact on climate conditions across its influence on the growth and physiology of plants [8, 9]. In the presence of elevated CO_2 levels, plants experience an increase in photosynthetic carbon fixation rates, even with reduced or maintained stomatal aperture. This phenomenon, known as CO_2 fertilization, leads to enhanced biomass production [10, 11]. Additionally, the effects of non-radiative in higher CO_2 scenario cause a reduction of conductance and transpiration in stoma, which is referred to as CO_2 physiological forcing.[12, 13]. The effects of enhanced CO_2 on plants vary depending on the species and environmental conditions, and studies indicate that these effects can have contrasting impacts on climate [14, 15]. While the influence of CO_2 fertilization on leaf area index (LAI) is often limited, it can result in increased LAI during early plant development and in regions with water limitations, particularly in nutrient-limited areas and mature forests [16, 17]. Increased leaf area index (LAI) promotes higher rates of plant transpiration and enhances surface evaporative cooling., provided there is sufficient moisture supply [18]. However, in regions where water limitation is not severe, CO_2 physiological forcing reduces transpiration. As a consequence, the ratio of sensible to latent heat fluxes at the leaf surface is increased, consequently raising the temperature of boundary layer [19, 20].

Considering the influence of both CO_2 physiological forcing and CO_2 fertilization, which are commonly referred to as CO_2 vegetation forcing, it is evident that they have an impact on surface moisture and energy fluxes. As a result, both of these factors may contribute to the occurrence of extreme events. [21–23]. However, the overall effects on projected extreme events are still uncertain. For example, elevated CO_2 levels could lead to a vegetation response that mitigates the the occurrence and severity of summer heat waves [24, 25]. This could occur through increased canopy water use efficiency (WUE, the ratio of carbon assimilation rate to transpiration rate) during springtime, which is induced by CO_2 physiological forcing. This would subsequently increase soil-moisture availability for cooling effcts due to evapotranspiraion later in the summer peak [26]. Additionally, the increase in atmospheric CO_2 concentrations, together with other greenhouse gases, is anticipated to lead to substantial alterations in evaporation patterns (over oceans) and evapotranspiration (over land) through enhanced radiative forcing [27]. Additionally, elevated CO_2 concentrations can cause changes in evapotranspiration unrelated to radiative forcing. In the presence of elevated CO_2 levels, many plant species reduce transpiration and conductance in stoma rates to minimize water loss, as observed in numerous plant species. Consequently, this adaptation results in an improvement in plant water use efficiency. [28, 29]. These changes in transpiration can affect soil moisture and evapotranspiration, which in turn impact the intensity, duration, and frequency of precipitation events [30]. As transpiration accounts for approximately 64% of the terrestrial evapotranspiration [31], gaining insights into the intricate and occasionally contradictory reactions of vegetation-water interactions to fluctuations in CO_2 levels is crucial for global hydrologic cycle and energy assessment in the future [21].

The majority of research focused on future extreme events relies on climate model simulations, which typically consider either the radiative effect of CO_2 alone or incorporate both CO_2 radiative forcing and CO_2 physiological forcing along with CO_2 fertilization concurrently. [32]. Prior studies investigating CO_2 vegetation forcing have predominantly examined the average temperature response over annual or seasonal time scales. However, these investigations have not thoroughly explored the potential differential impacts of future CO_2 vegetation forcing on heat and precipitation extremes compared to the mean conditions [33–35]. In this study, we examine a set of Earth system models (ESMs) from the CMIP6 that incorporate active biogeophysics and biogeochemistry to investigate the impact of VEG (by increasing CO_2 concentrations fourfold) on extreme events of heat and precipitation in China.

The study is structured as follows: Section 2 outlines the data and methods used. Section 3 presents the main findings regarding the influence of vegetation forcing on extreme events. Finally, Section 4 offers concluding remarks and discusses the implications of our study.

2 Data and methods

2.1 Experiment design

We examined the roles of CO_2 radiative forcing and CO_2 vegetation forcing by utilizing simulations from five ESMs, which were obtained from the carbon-climate feedback experiment within CMIP6. The ESMs we selected for this study were CanESM2, CESM1-BGC, BCC-CSM1-1, IPSL-CM5A-LRand MPI-ESMLR. Because these models were chosen based on their daily-scale rainfall and temperature data, which were necessary for our analysis of precipitation and heat extremes. In order to evaluate the influence of VEG on climate, we conducted comparative simulations for each model. Two model runs were conducted for each model, one incorporating the comprehensive interactive effects of rising CO_2 levels on radiative forcing, physiological responses, and fertilization. (Total referred to as 1pctCO_2 in CMIP6, as shown in Table 1 and Fig. 2c). The concentration of CO_2 in this experiment is increasing in both the atmosphere and the carbon cycle on land and oceans. Further experiments carried out within the framework of the Coupled Climate-Carbon Cycle Model Intercomparison

Project (C4MIP, [36, 37]) allow us to distinguish the individual contributions of CO_2 vegetation forcing and radiative effects. A separate simulation solely considering the radiative effects of elevated CO_2 (RadCO_2, referred to as 1pctCO_2-rad in CMIP6, as shown in Table 1 and Fig. 1a). The simulations were divided into two sets, differing only in whether the model's vegetation was directly impacted by the rising CO_2 levels (RadCO_2) or not, which is crucial for our analysis. Alongside evaluating the impact of VEG on climate, we also assessed the influence of RAD. To achieve this, we compared the Total simulations with another set of simulations called VegCO_2 (see Table 1 and Fig. 1b), which focused exclusively on the physiological and fertilization impacts of heightened CO_2 levels and is denoted as 1pctCO_2-bgc in CMIP6. The two sets of simulations differ only in the direct influence of increasing CO_2 on the atmospheric radiative transfer scheme in VegCO_2. It is important to note that we utilize the RadCO_2 to isolate the impact of VEG on climate (i.e., VEG = Total - RadCO_2), while the VegCO_2 simulations are used to isolate the influence of RAD(i.e., RAD = Total - VegCO_2).

In all simulation sets, the CO_2 concentrations gradually rise by 1% per year over a span of 140 years, commencing at 284 ppm and reaching approximately 1132 ppm at the end (Table 2) [21, 38]. We concentrate on extreme events across various CO_2 concentration scenarios. The $1\times CO_2$ period is from year 1 to year 29, with an average CO_2 concentration of around 330 ppm. The $2\times CO_2$ period is from year 58 to year 87, with an average CO_2 concentration of about 575 ppm. The $4\times CO_2$ period is from year 111 to year 140, with an average CO_2 concentration of roughly 984 ppm. The reference climate used for defining extremes is the period from year 1 to year 29 in the Total simulation. All the data is remapped to $1°\times1°$.

Table 1 Summary of the employed CMIP6 experiments.

Simulation name	CMIP6 experiment name	Effects of CO_2 concentration on Land	Effects of CO_2 concentration on Atmosphere
Total	1pctCO_2	1% per year	1% per year
RadCO_2	1pctCO_2-rad	Pre-industrial	1% per year
VegCO_2	1pctCO_2-bgc	1% per year	Pre-industrial

Table 2 CO_2 forcing experiment.

Experiment	Time range	Reference climate for extreme heat and precipitation definition
$1\times CO_2$	Years of 1-29	Years of 1-29 in Total
$2\times CO_2$	Years of 58-87	
$4\times CO_2$	Years of 111-140	

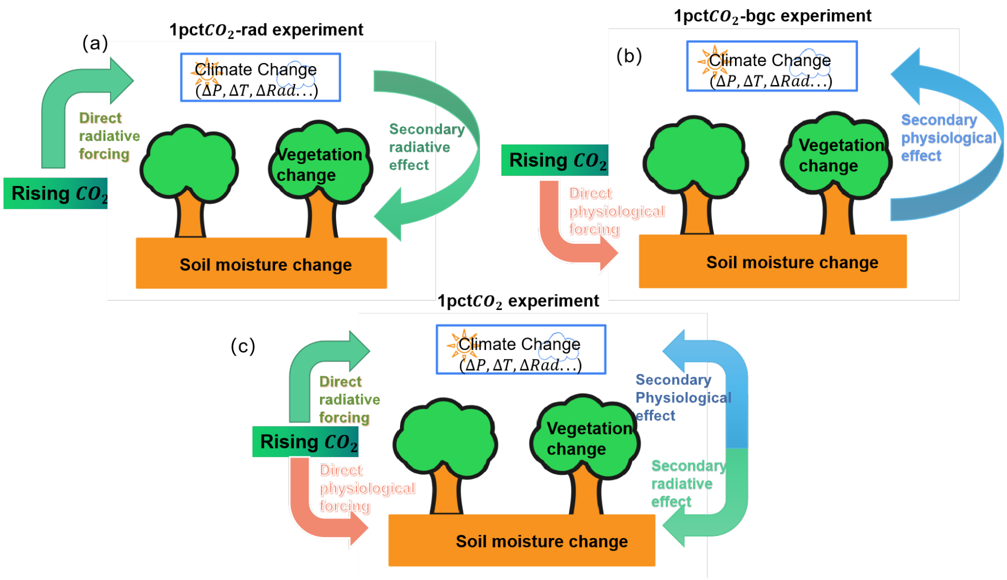

Fig. 1 Descriptions of the direct and secondary effects of CO_2 radiative and physiological forcings in CMIP6 simulations: (a) In the expriment of 1pctCO_2-rad, only RAD is considered, which involves the effects of enhanced atmospheric CO_2 concentration on radiative transfer processes and climate. The direct radiative forcing leads to changes in climate variables such as net radiation (Rad), air temperature (T), precipitation (P) and others, directly influencing the terrestrial water cycle and energy. These climatic changes further affect soil moisture and vegetation cover, leading to an additional radiative effect that modifies how precipitation is distributed between evapotranspiration and energy exchange at the land surface. (b) In the 1pctCO_2-bgc experiment, only CO_2 physiological forcing is considered, focusing on the influence of increased atmospheric CO_2 concentration on plant physiological behavior. The direct physiological forcing entails the response of vegetation to elevated CO_2, influencing transpiration, evaporation from canopy interception and soils, primarily through the reduction in stomatal conductance and increase in vegetation cover. These CO_2-induced changes in evapotranspiration alter the interactions between land and atmosphere in terms of water and energy exchanges, atmospheric circulation, precipitation, and potential evapotranspiration (PET), leading to additional impacts on the terrestrial water balance. (c) The experiment of 1pctCO_2 includes both radiative and physiological forcings of rising CO_2 concentration, encompassing the combined effects described in (a) and (b).

2.2 Extreme events definition

2.2.1 Heat wave detection

The study examines heat waves using the temperature extreme indices recommended by the World Meteorological Organization (WMO) [39]. In particular, A heatwave event is characterized as a duration of at least three consecutive days when the maximum temperature surpasses the 90th percentile value of the daily maximum temperature for the corresponding calendar day in a reference period, which is determined by a 5-day moving average [40]. To consider the effects of seasonality and temporal autocorrelation in the daily data, a percentile is obtained for each calendar day and we also use a 5-day moving average on the dataset. We utilize four metrics to analyze extreme heat events: HWTD (Heat wave total days), representing the total number of days meeting the heat wave criteria in each season. HWML (Heat wave max length), indicating the length of the longest heat wave event in each season. HWN (Heat wave number), epresenting the average amount of heat wave occurrences per season. HWMI (Heat wave max intensity), representing the highest daily temperature reached once each heat wave event occurred. We then calculate the 30-year average of these four metrics annually.

2.2.2 Precipitation detection

Extreme precipitation is determined by identifying heavy rainy days that surpass the 95th percentile observed during the reference period. Conversely, a dry day is defined as having no precipitation if the accumulated daily rainfall amounts to less than 0.1 mm within a year [21]. Maximum 1-day precipitation (RX1day) is an indicator that measures extreme precipitation events and is defined as the maximum of single-day maximum precipitation. This indicator is commonly used to study the relationship between climate change and extreme weather events, as extreme precipitation events may increase in frequency and intensity as a result of climate change. RX1day is one of the extreme climate indices of the WMO and is widely used in climate simulation and prediction. In this paper, we use the index of extreme precipitation RX1day to represent the annual extreme precipitation events that have significant impacts on society.

2.3 Significance test

We generated a multi-model ensemble (MME) by converting the outputs of the Earth System Models (ESMs) to a consistent $1^{\circ}\times1^{\circ}$ grid. To assess the significance of differences between the experiments, we utilized the bootstrap method. Within the MME, we randomly sampled 5 values from the 5 ESMs with replacement, computed their average, repeated this process 1000 times, established confidence intervals, and reported only the 95% significant values to represent the consensus among the models..

3 Results

3.1 Precipitation

We examined precipitation in three scenarios, namely $1\times CO_2$, $2\times CO_2$, and $4\times CO_2$. During the $1\times CO_2$ period, which spans from year 1 to year 29 and features an average CO_2 concentration of about 330 ppm. It has been researched that CO_2 has a significant impact on the early growth of LAI and in areas with water scarcity [22]. When water supply is sufficient, a higher LAI can increase plant transpiration and surface evaporation cooling. At the same time, in areas where water supply is not severely restricted (humid areas), CO_2 physiological forcing reduces transpiration and increases the ratio of sensible heat flux to latent heat flux, thus increasing leaf surface temperature. This leads to an increase in boundary layer temperature. Dry soil and low transpiration increase surface temperatures during heat waves. Based on the previous researches, we divided China into two areas based on the Aridity Index (AI). Regions with an AI less than 0.65 were designated as dry areas, while those with an AI greater than 0.65 were designated as humid areas (humid area). By utilizing this separation approach, we were able to specifically isolate the impacts of CO_2 vegetation forcing on these two regions. We found that the vegetation forcing led to a drying trend in China overall (-6.43 ± 1.55; mean ± s.d., Fig. 2a), with humid area becoming even drier (12.92 ± 3.54) and dry area becoming slightly wetter (0.058 ± 0.012). On the other hand, the radiative forcing resulted in increased precipitation across China (18.76 ± 5.52, Fig. 2d). The $2\times CO_2$ period, which occurred from year 58 to year 87 and had an average CO_2 concentration of approximately 575 ppm, led to a drying effect on all of China due to vegetation forcing (-9.89 ± 1.06, Fig. 2b), with both humid area (-17.53 ± 4.56) and dry area (2.37 ± 0.58) experiencing reduced precipitation. Once again, the radiative forcing led to increased precipitation across China (27.93 ± 6.52, Fig. 2e). Finally, during the $4\times CO_2$ period from year 111 to year 140, with an average CO_2 concentration of about 984 ppm, the vegetation forcing caused drying across all of China (-5.72 ± 1.23, Fig. 2c), with both humid area (-5.74 ± 1.26) and dry area (-5.69 ± 1.38) experiencing a decline in precipitation. However, the radiative forcing led to increased precipitation across China (27.93 ± 6.52, Fig. 2f).

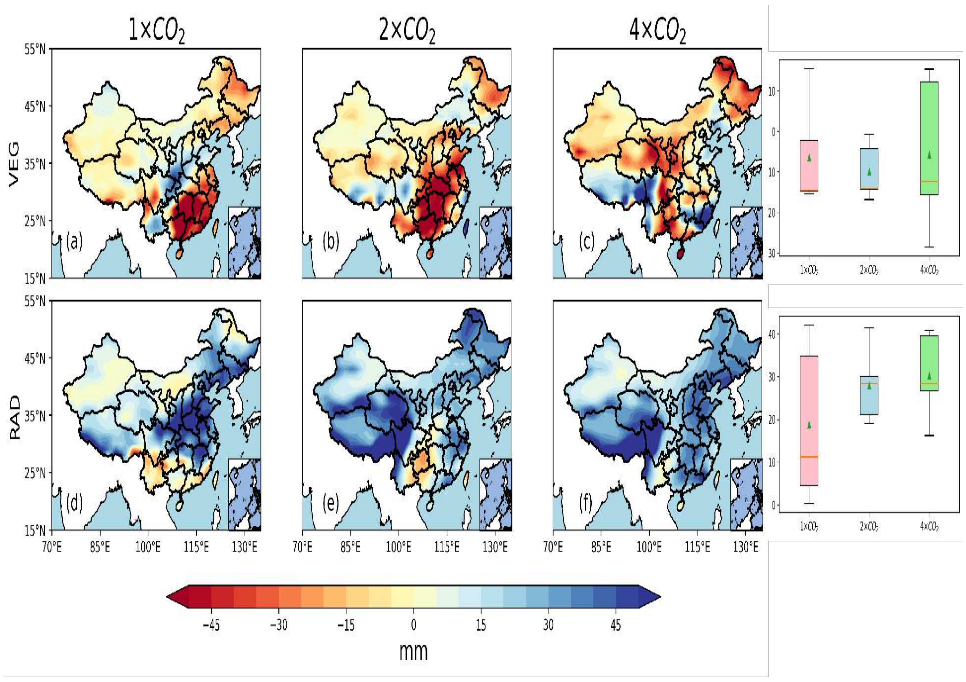

Fig. 2 Effects of CO_2 vegetation forcing (VEG) and radiative forcing (RAD) on mean precipitation. The right column is the variations in the precipitation of VEG and RAD. Only statistically significant differences are shown.

We conducted an analysis of how CO_2 vegetation forcing (VEG) affects the 95th extreme precipitation in China. Our findings indicate that VEG tends to reduce heavy rainfall, with negative responses observed in all three scenarios (-0.14 ± 0.033, -0.15 ± 0.028, -0.52 ± 0.041; Fig. 3a-c). Conversely, radiative forcing (RAD) tends to promote the 95th extreme precipitation (1.18 ± 0.26, 4.43 ± 0.53, 9.24 ± 1.35; Fig. 3d-f).

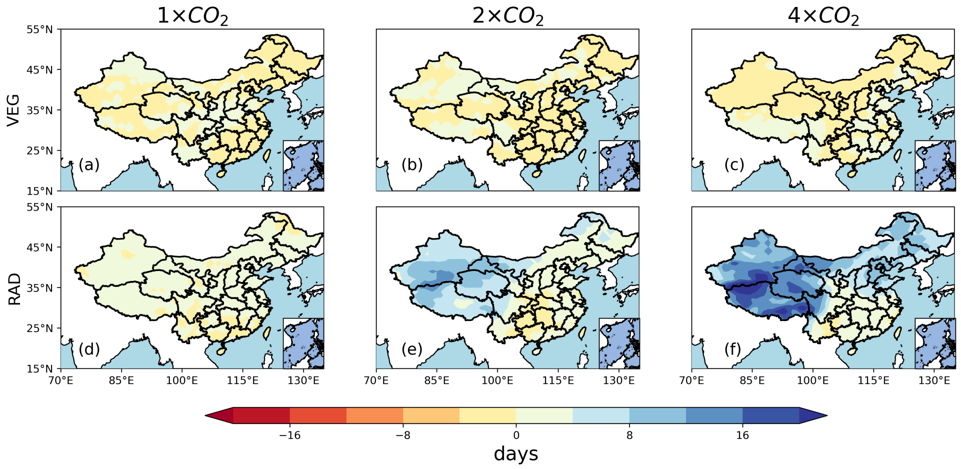

Fig. 3 Effects of VEG and RAD on 95th extreme precipitation. Only statistically significant differences are shown.

Additionally, we calculated the effects of VEG on the trend of days with extreme precipitation exceeding the 95th percentile (Fig. 4). In the $1\times CO_2$ scenario, VEG resulted in a decreasing trend, with a slope of -0.12 day/decade (Fig. 4a). In the $2\times CO_2$ and $4\times CO_2$ scenarios, the trends were 0.11 and -0.17 day/decade, respectively. Only in the $2\times CO_2$ scenario did VEG contribute to an increasing trend. Regarding radiation (RAD), both the $1\times CO_2$ and $2\times CO_2$ scenarios exhibited decreasing trends (-0.006 and -0.019 days/decade, Fig. 4b). In the $4\times CO_2$ scenario, RAD leds to an enhancement in the trend of days with extreme precipitation exceeding the 95th percentile, with a trend of 0.32 day/decade.

We classified a dry day as a day with negligible precipitation, specifically when the accumulated daily rainfall amounted to less than 0.1 mm over the course of one year. From $1\times CO_2$ to $4\times CO_2$, VEG results in more dry days (0.28 ± 0.053, 1.53 ± 0.095, 3.47 ± 0.26; Fig. 5a-c). From $1\times CO_2$ to $4\times CO_2$, VEG leads to fewer dry days (-1.33 ± 0.088, -2.52 ± 0.13, -3.84 ± 0.26; Fig. 5d-f). There are noticeable differences between humid area and dry area in the RAD effects of $2\times CO_2$ and $4\times CO_2$. In $2\times CO_2$ (Fig. 5e), RAD results in fewer dry days in dry area (-6.47 ± 1.22) and more dry days in humid area (1.49 ± 0.15). Furthermore, the difference is more apparent in $4\times CO_2$ (Fig. 5f), with RAD leading to fewer dry days in dry area (-9.78 ± 2.62) and more dry days in humid area (2.18 ± 0.37).

The RX1day is a metric utilized to assess extreme precipitation events, often used to examine the connection between climate change and extreme weather. With climate change, extreme precipitation events may become more frequent and severe. In this study, we computed the RX1day and illustrated its trend (mm/yr) in Fig. 6. Results

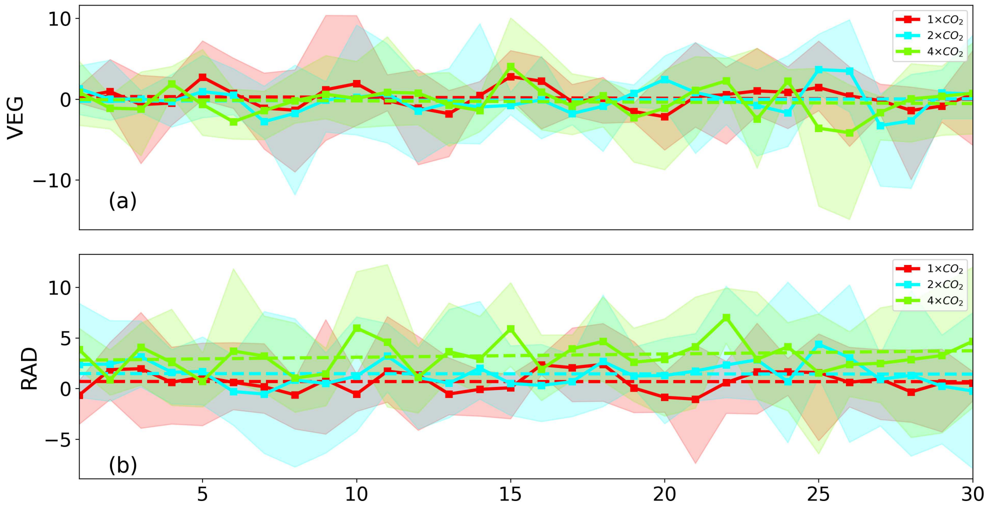

Fig. 4 Effects of VEG and RAD on the trend of days that exceed 95th extreme precipitation. The red dotted line is ensemble mean of the 1×CO_2.trend The cyan and green are 2×CO_2 and 4×CO_2. The shading areas are the uncertainties. (a) is the VEG and (b) is the RAD.

indicate that from 1×CO_2 to 4×CO_2, the trends caused by China's VEG are 0.051 ± 0.0058, -0.013 ± 0.0069, 0.045 ± 0.015 (Fig. 6a-c). The trends in humid area were more responsive to VEG than in dry area, where VEG tends to decrease the trend. Specifically, in humid area, the VEG-induced trends are 0.073 ± 0.015, -0.043 ± 0.0091, and 0.037 ± 0.0083. Moreover, the trends induced by RAD are 0.11 ± 0.095, 0.063 ± 0.0086, and 0.15 ± 0.067 in the 1×CO_2, 2×CO_2, and 4×CO_2 scenarios, respectively.

3.2 Heat wave

Carbon dioxide, as a prominent greenhouse gas contributing to global warming, also plays a beneficial role in enhancing vegetation's carbon uptake capacity, which serves as a partial offset to emissions. However, the physiological response of vegetation to increasing carbon dioxide, such as partial closure of stomata and an increase in leaf area, can actually exacerbate global warming. Unfortunately, this effect is often neglected in assessments of climate change mitigation strategies. In fact, the physiological response of vegetation to rising carbon dioxide consistently amplifies the warming effect, mainly due to the reduction in evapotranspiration caused by stomatal closure [22]. In this section, we conduct the analysis on the effects of CO_2 vegetation forcing on Chinese heat wave event.

From Fig. 7, it is evident that VEG has caused an increase in the mean temperature except in the case of 1×CO_2. When comparing the temperature changes induced by VEG from 1×CO_2 to 4×CO_2 (Fig. 7a-c), it can be observed that they are -0.011 ± 0.006, 0.099 ± 0.015, and 0.44 ± 0.24, respectively. Both dry area and humid area experience warmer temperatures due to VEG for 2×CO_2 and 4×CO_2. Additionally, RAD could contribute to warming in China, with mean temperature changes induced

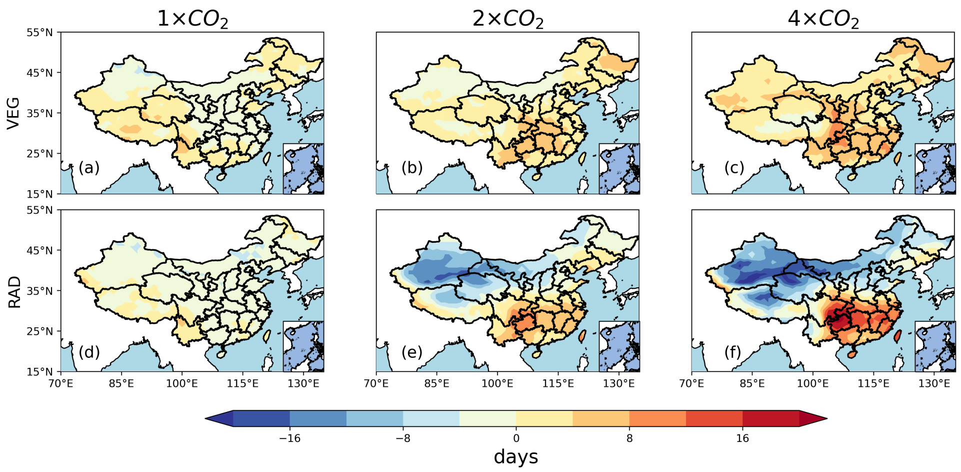

Fig. 5 Effects of VEG and RAD on number of dry days. We established a definition for a dry day as a day without any precipitation when the total amount of daily precipitation is below 0.1 mm within a year. Only statistically significant differences are shown.

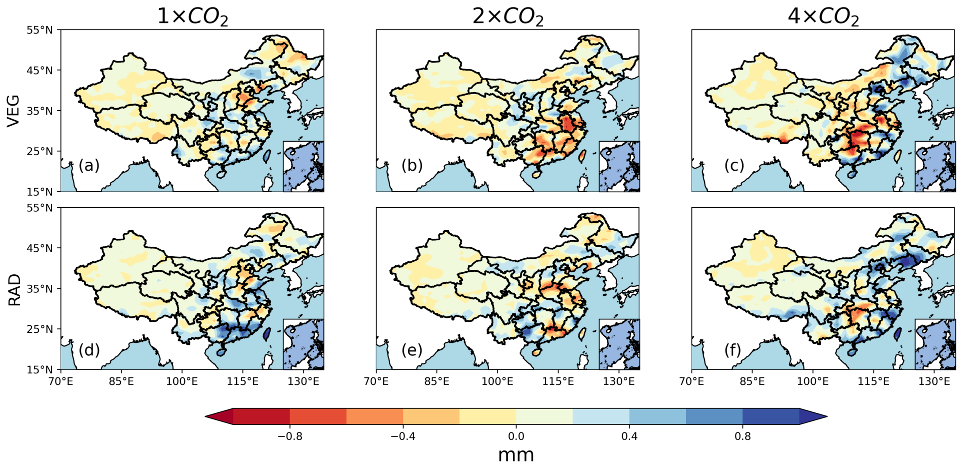

Fig. 6 Effects of VEG and RAD on number of dry days. We established a definition for a dry day as a day without any precipitation when the total amount of daily precipitation is below 0.1 mm within a year. Only statistically significant differences are shown.

by RAD being 0.51 ± 0.13, 0.52 ± 0.15, and 0.58 ± 0.11, respectively. The CO_2 vegetation forcing and radiative forcing have had the most significant impact on temperature changes.

Four metrics are used to analyze extreme heat events: HWN, which represents the average number of heat waves per season; HWTD, which is the total number of days that meet the heat wave criteria in each season; HWML, which measures the length of the longest heat wave event in each season; and HWMI, which represents the maximum daily temperature reached during each heat wave event. Although VEG increases the

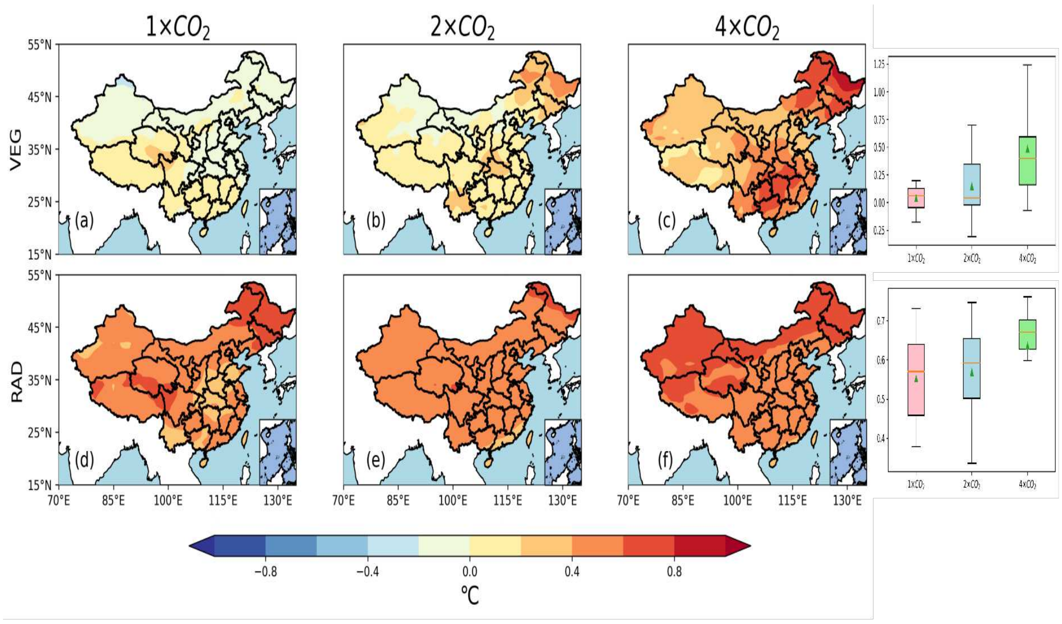

Fig. 7 Effects of VEG and RAD on mean temperature. The right column is the variations in the precipitation of VEG and RAD. Only statistically significant differences are shown.

mean temperature, it has a negative effect on the number of heat waves. From $1\times CO_2$ to $4\times CO_2$ (Fig. 8a-c), the heat wave number induced by VEG decreases (-0.54 ± 0.12, -0.18 ± 0.054, and -0.58 ± 0.13, respectively). Conversely, RAD causes an increase in HWN except in $1\times CO_2$ (-0.017 ± 0.0054, 1.48 ± 0.39, 1.79 ± 0.42; Fig. 8d-f).

Additionally, we calculated the effects of VEG on trend of heat wave number(Fig. 9). In the $1\times CO_2$ and $2\times CO_2$ scenarios, VEG resulted in a decreasing trend, with a slope of 0.03 and 0.02 event/decade, respectively(Fig. 9a). In the $4\times CO_2$ scenario, the trends were -0.01 event/decade. Only in the $4\times CO_2$ scenario did VEG contribute to an decreasing trend. Regarding radiation (RAD), both the $1\times CO_2$ and $2\times CO_2$ scenarios exhibited increasing trends (0.46 and 0.22 event/decade, Fig. 9b). In the $4\times CO_2$ scenario, RAD led to an decrease in the trend of days with heat wave number, with a trend of -0.41 event/decade.

Regarding HWTD (Fig. 10), VEG increases the total days of heat wave in $2\times CO_2$ and $4\times CO_2$. Specifically, the additional days induced by VEG are - 0.69 ± 0.24, 2.48 ± 1.11, and 5.45 ± 2.57 (Figure 10a-c). VEG has a stronger effect on humid area than on dry area. In comparison, RAD has a more intense impact and leads to more heat wave days (3.25 ± 1.22, 2.94 ± 0.95, 7.09 ± 3.55). Both VEG and RAD have a greater influence on humid area than dry area.

Regarding HWML (Fig. 11), both VEG and RAD make the longest heat wave events longer in $2\times CO_2$ and $4\times CO_2$. The additional days induced by VEG from $1\times CO_2$ to $4\times CO_2$ are -0.49 ± 0.21, 1.06 ± 0.45, and 2.69 ± 1.13, respectively. RAD prolongs the heat wave events more than VEG. Additionally, for HWMI (Fig. 12),

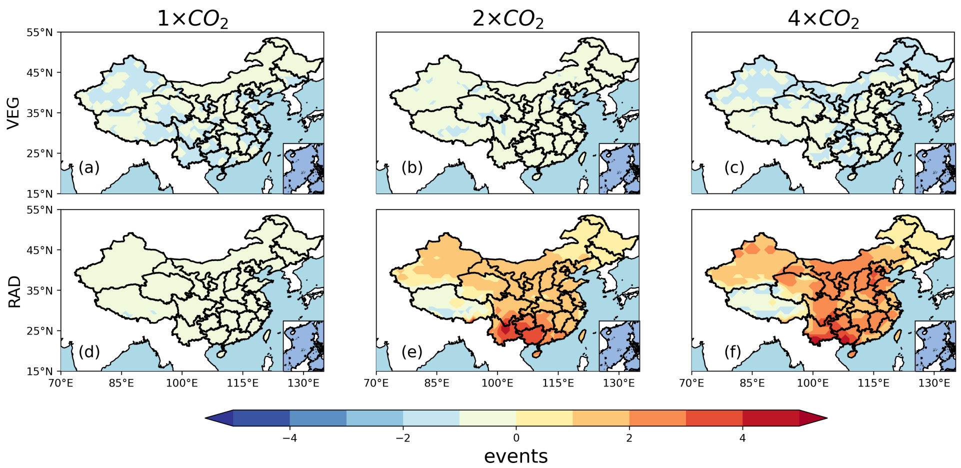

Fig. 8 Effects of VEG and RAD on mean temperature. The right column is the variations in the precipitation of VEG and RAD. Only statistically significant differences are shown.

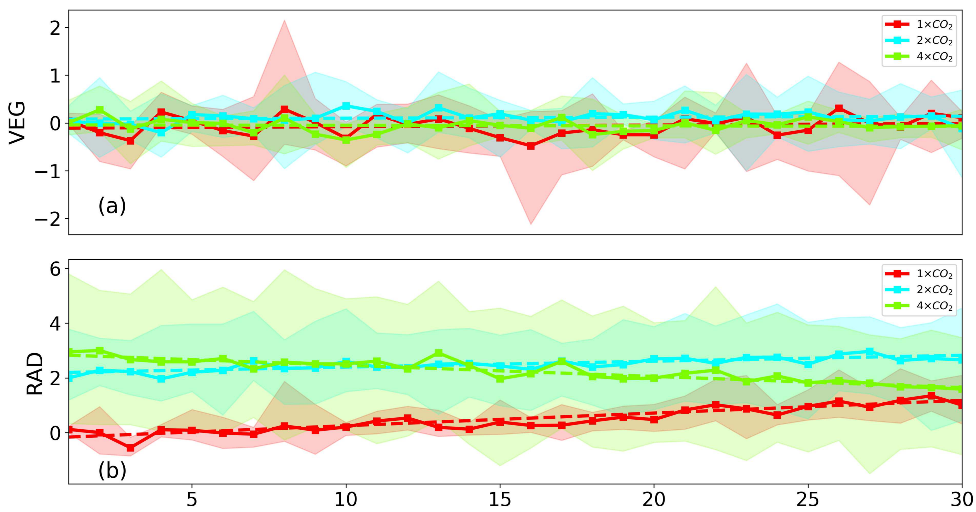

Fig. 9 Effects of VEG and RAD on the trend of heat wave number (HWN). The red dotted line is ensemble mean of the $1\times CO_2$.trend The cyan and green are $2\times CO_2$ and $4\times CO_2$. The shading areas are the uncertainties. (a) is the VEG and (b) is the RAD.

both VEG and RAD make the intensity of heat waves stronger. The average maximum temperature increase induced by VEG is 0.14 ± 0.056, 0.51 ± 0.21, and 0.60 ± 0.29, respectively. For RAD, the corresponding figures are 2.18 ± 1.22, 2.61 ± 1.25, and 3.47 ± 1.99. Furthermore, both RAD and VEG have a stronger impact on humid area than on dry area.

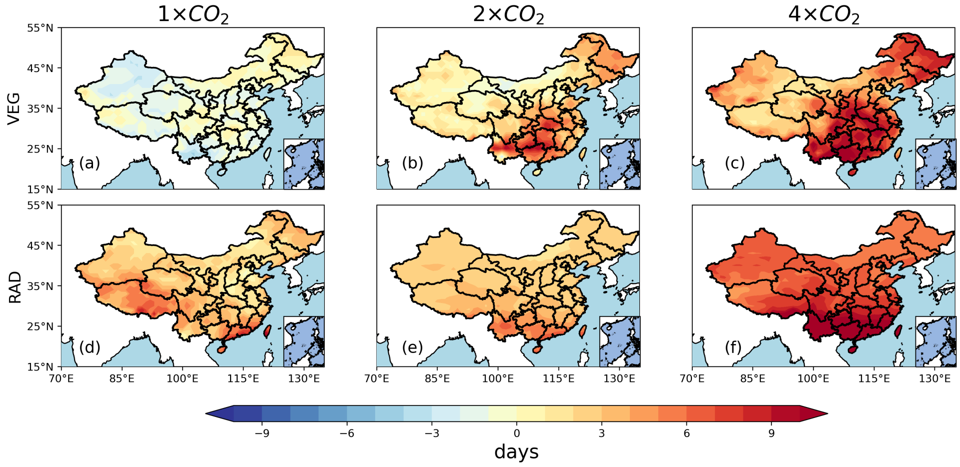

Fig. 10 Effects of VEG and RAD on total heat wave days (HWTD). Only statistically significant differences are shown.

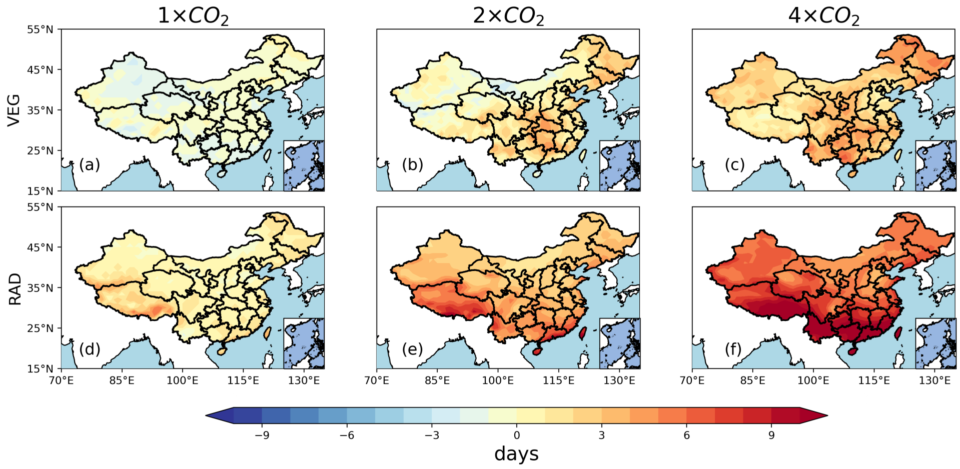

Fig. 11 Effects of VEG and RAD on heat wave maximum length (HWML). Only statistically significant differences are shown.

4 Conclusions and discussion

Theoretical studies and climate models suggest that rising concentrations of CO_2 will bring substantial changes to global precipitation and temperature patterns [41]. As a result, due to the rise in CO_2 levels, it is anticipated that the occurrence of extreme heat events will witness a substantial increase in the upcoming decades. While most projections of future extreme events mainly focus on the radiative effects of CO_2, our findings indicate that the direct impact of rising atmospheric CO_2 concentrations on temperature and precipitation in vegetated regions of China, known as CO_2 vegetation

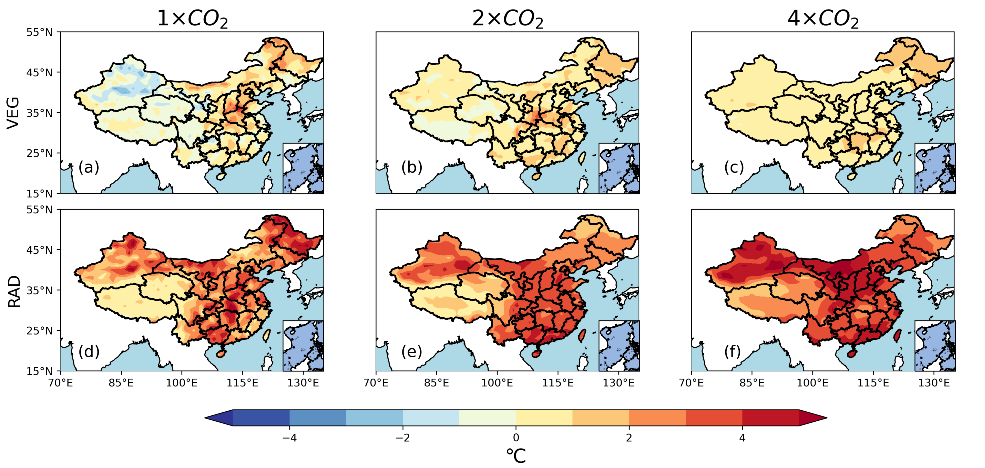

Fig. 12 Effects of VEG and RAD on heat wave maximum intensity (HWMI). Only statistically significant differences are shown.

forcing, should not be overlooked. Despite the enhanced leaf area index (LAI) resulting from elevated CO_2, the reduction in stomatal conductance during the warm season due to CO_2 physiological forcing limits surface evaporative cooling and contributes to an upward shift in both average and extreme summer temperatures in China. The decrease in transpiration caused by CO_2 physiological forcing triggers various interactions among climate systems that further intensify the probability and severity of extreme heat events. The transition from latent to sensible heating leads to a drier and more stable boundary layer characterized by lower evapotranspiration (ET) and increased planetary boundary layer heights. Additionally, CO_2 vegetation forcing significantly reduces transpiration in vegetated areas of China, which may potentially lead to an increase in the frequency of dry days. The days that exceed the 95th extreme precipitation decrease in the near future. In different CO_2 scenarios, the VEG and RAD show various effects on extreme events. All in all, these physiologically driven changes can either amplify or mitigate the effects of radiative forcing on future precipitation patterns. Overall, our findings highlight the particularly pronounced effects of CO_2 vegetation forcing in the humid regions of China across various scenarios.

In the current climate, the analysis of CMIP6 experiments in this study highlights the significant role of CO_2 vegetation forcing in hydrological and energy processes. However, under high-CO_2 conditions, the reduction in transpiration resulting from CO_2 physiological forcing outweighs the potential increase in transpiration from CO_2 fertilization. This leads to a widespread increase in heat waves and a decrease in extreme precipitation in China. Even after anthropogenic CO_2 emissions cease, temperatures and heat extremes will continue to rise due to the thermal inertia in the oceans. It is crucial to enhance our understanding of the influence of vegetation on carbon and hydrologic cycles and develop improved models to better anticipate and mitigate the severe impacts of future heat waves. This is particularly important considering the potential of plant changes to influence the surface energy and hydrological cycle in the future.

Acknowledgments. We thank Prof. Qian help for polishing the this manuscript. We thank Dr. Fan and Hou for providing the the data and script. We thank Prof. Sun and Feng for designing the idea of this study.

Declarations

The authors declare that they have no confict of interest

- Funding
This study was especially supported by the National Natural Science Foundation of China under Grant nos.41975062. This study was also funded by the National Natural Science Foundation of China under Grant nos. 42130610, 42275034, 42075029, 41675050, and 11801398 and the Outstanding Young Talents Support Plan of Shanxi province. This work was also funded by Gansu Provincial Science and Technology Project under Grant nos. 22JR5RA405.
- Authors' contributions
Z. Chen and X.T. Hou helped design the study. X.T. Hou, P.Y. Fan and F. Ji accessed and processed the dataset. They also helped to write the manuscript. L. Li and Z.H. Qian helped to contribute the writing. G.Q. Sun and G.L. Feng helped with validations. The finished version of the manuscript has been reviewed and get all the approvals from all authors.
- Data availability
The CMIP6 data is available for access at the following URL: https://esgf-node.llnl.gov/search/cmip6/.

References

[1] Semenza, J. C. *et al.* Heat-related deaths during the july 1995 heat wave in chicago. *New England journal of medicine* **335**, 84–90 (1996).

[2] Fouillet, A. *et al.* Excess mortality related to the august 2003 heat wave in france. *International archives of occupational and environmental health* **80**, 16–24 (2006).

[3] Frank, D. *et al.* Effects of climate extremes on the terrestrial carbon cycle: concepts, processes and potential future impacts. *Global change biology* **21**, 2861–2880 (2015).

[4] García-Herrera, R., Díaz, J., Trigo, R. M., Luterbacher, J. & Fischer, E. M. A review of the european summer heat wave of 2003. *Critical Reviews in Environmental Science and Technology* **40**, 267–306 (2010).

[5] Ciais, P. *et al.* Europe-wide reduction in primary productivity caused by the heat and drought in 2003. *Nature* **437**, 529–533 (2005).

[6] Sun, Y. & Ding, Y. A projection of future changes in summer precipitation and monsoon in east asia. *Science China Earth Sciences* **53**, 284–300 (2010).

[7] Sun, Y. *et al.* Rapid increase in the risk of extreme summer heat in eastern china. *Nature Climate Change* **4**, 1082–1085 (2014).

[8] Lammertsma, E. I. *et al.* Global co2 rise leads to reduced maximum stomatal conductance in florida vegetation. *Proceedings of the National Academy of Sciences* **108**, 4035–4040 (2011).

[9] Keenan, T. F. *et al.* Increase in forest water-use efficiency as atmospheric carbon dioxide concentrations rise. *Nature* **499**, 324–327 (2013).

[10] Cowling, S. A. & Field, C. B. Environmental control of leaf area production: implications for vegetation and land-surface modeling. *Global Biogeochemical Cycles* **17**, 7–1 (2003).

[11] Zhu, Z. *et al.* Greening of the earth and its drivers. *Nature climate change* **6**, 791–795 (2016).

[12] Sellers, P. J. *et al.* A revised land surface parameterization (sib2) for atmospheric gcms. part ii: The generation of global fields of terrestrial biophysical parameters from satellite data. *Journal of climate* **9**, 706–737 (1996).

[13] Betts, R. A. *et al.* Projected increase in continental runoff due to plant responses to increasing carbon dioxide. *Nature* **448**, 1037–1041 (2007).

[14] Kergoat, L. *et al.* Impact of doubled co2 on global-scale leaf area index and evapotranspiration: Conflicting stomatal conductance and lai responses. *Journal of Geophysical Research: Atmospheres* **107**, ACL–30 (2002).

[15] Ainsworth, E. A. & Long, S. P. What have we learned from 15 years of free-air co2 enrichment (face)? a meta-analytic review of the responses of photosynthesis, canopy properties and plant production to rising co2. *New phytologist* **165**, 351–372 (2005).

[16] Warren, J. M. *et al.* Ecohydrologic impact of reduced stomatal conductance in forests exposed to elevated co2. *Ecohydrology* **4**, 196–210 (2011).

[17] Donohue, R. J., Roderick, M. L., McVicar, T. R. & Farquhar, G. D. Impact of co2 fertilization on maximum foliage cover across the globe's warm, arid environments. *Geophysical Research Letters* **40**, 3031–3035 (2013).

[18] Swann, A. L., Hoffman, F. M., Koven, C. D. & Randerson, J. T. Plant responses to increasing co2 reduce estimates of climate impacts on drought severity. *Proceedings of the National Academy of Sciences* **113**, 10019–10024 (2016).

[19] Cao, L., Bala, G., Caldeira, K., Nemani, R. & Ban-Weiss, G. Importance of carbon dioxide physiological forcing to future climate change. *Proceedings of the National Academy of Sciences* **107**, 9513–9518 (2010).

[20] Fatichi, S. *et al.* Partitioning direct and indirect effects reveals the response of water-limited ecosystems to elevated co2. *Proceedings of the National Academy of Sciences* **113**, 12757–12762 (2016).

[21] Skinner, C. B., Poulsen, C. J., Chadwick, R., Diffenbaugh, N. S. & Fiorella, R. P. The role of plant co2 physiological forcing in shaping future daily-scale precipitation. *Journal of Climate* **30**, 2319–2340 (2017).

[22] Skinner, C. B., Poulsen, C. J. & Mankin, J. S. Amplification of heat extremes by plant co2 physiological forcing. *Nature Communications* **9**, 1094 (2018).

[23] Park, S.-W., Kim, J.-S. & Kug, J.-S. The intensification of arctic warming as a result of co2 physiological forcing. *Nature communications* **11**, 2098 (2020).

[24] Field, C., Lund, C., Chiariello, N. & Mortimer, B. Co2 effects on the water budget of grassland microcosm communities. *Global Change Biology* **3**, 197–206 (1997).

[25] Medlyn, B. E. *et al.* Stomatal conductance of forest species after long-term exposure to elevated co2 concentration: a synthesis. *New Phytologist* **149**, 247–264 (2001).

[26] Lemordant, L., Gentine, P., Swann, A. S., Cook, B. I. & Scheff, J. Critical impact of vegetation physiology on the continental hydrologic cycle in response to increasing co2. *Proceedings of the National Academy of Sciences* **115**, 4093–4098 (2018).

[27] Milly, P. C. & Dunne, K. A. Potential evapotranspiration and continental drying. *Nature Climate Change* **6**, 946–949 (2016).

[28] Chen, Z., Wu, Y.-P., Feng, G.-L., Qian, Z.-H. & Sun, G.-Q. Effects of global warming on pattern dynamics of vegetation: Wuwei in china as a case. *Applied Mathematics and Computation* **390**, 125666 (2021).

[29] Chen, Z. *et al.* Effects of climate change on vegetation patterns in hulun buir grassland. *Physica A: Statistical Mechanics and its Applications* **597**, 127275 (2022).

[30] Lee, J.-E. *et al.* Reduction of tropical land region precipitation variability via transpiration. *Geophysical Research Letters* **39** (2012).

[31] Good, S. P., Noone, D. & Bowen, G. Hydrologic connectivity constrains partitioning of global terrestrial water fluxes. *Science* **349**, 175–177 (2015).

[32] Sillmann, J., Kharin, V. V., Zwiers, F. W., Zhang, X. & Bronaugh, D. Climate extremes indices in the cmip5 multimodel ensemble: Part 2. future climate projections. *Journal of geophysical research: atmospheres* **118**, 2473–2493 (2013).

[33] Kitoh, A. *et al.* Monsoons in a changing world: A regional perspective in a global context. *Journal of Geophysical Research: Atmospheres* **118**, 3053–3065 (2013).

[34] Lee, J.-Y. & Wang, B. Future change of global monsoon in the cmip5. *Climate Dynamics* **42**, 101–119 (2014).

[35] Cui, J. *et al.* Vegetation forcing modulates global land monsoon and water resources in a co2-enriched climate. *Nature communications* **11**, 5184 (2020).

[36] Friedlingstein, P. *et al.* Climate–carbon cycle feedback analysis: results from the c4mip model intercomparison. *Journal of climate* **19**, 3337–3353 (2006).

[37] Jones, C. D. *et al.* C4mip–the coupled climate–carbon cycle model intercomparison project: Experimental protocol for cmip6. *Geoscientific Model Development* **9**, 2853–2880 (2016).

[38] Bathiany, S., Claussen, M. & Brovkin, V. Co2-induced sahel greening in three cmip5 earth system models. *Journal of Climate* **27**, 7163–7184 (2014).

[39] Zhang, X. *et al.* Indices for monitoring changes in extremes based on daily temperature and precipitation data. *Wiley Interdisciplinary Reviews: Climate Change* **2**, 851–870 (2011).

[40] Perkins, S. E. & Alexander, L. V. On the measurement of heat waves. *Journal of climate* **26**, 4500–4517 (2013).

[41] Trenberth, K. E., Dai, A., Rasmussen, R. M. & Parsons, D. B. The changing character of precipitation. *Bulletin of the American Meteorological Society* **84**, 1205–1218 (2003).